

A unified scalar-field resolution of the H_0 , S_8 and evolving Dark Energy tensions

Gerasimos Kouniatis^{1,2,*}

¹*Physics Department, National Technical University of Athens, 15780 Zografou Campus, Athens, Greece*

²*National Observatory of Athens, Lofos Nymfon, 11852 Athens, Greece*

We propose a unified scalar-field framework that addresses, within standard general relativity, three current cosmological anomalies: the H_0 tension, the mild preference for reduced late-time clustering (S_8), and recent indications of evolving dark energy. The model contains a single minimally coupled canonical scalar field evolving in a smooth potential composed of a localized bump superimposed on an exponential tail. The bump generates a transient pre-recombination energy injection that increases the expansion rate before last scattering, reduces the sound horizon, and shifts the CMB-inferred value of H_0 upward. After the field is released, its energy density rapidly redshifts through a kination-like phase, ensuring that the early modification does not persist as an unwanted late-time contribution. At low redshift, the exponential tail drives quintessence-like evolution, naturally yielding $w_0 > -1$ and $w_a < 0$ while suppressing linear structure growth and moving S_8 in the observationally preferred direction. The analysis shows explicitly how this smooth single-field potential can produce the required sequence of early enhancement, rapid dilution, and late-time thawing behavior.

I. INTRODUCTION

The spatially flat Λ CDM model continues to provide an excellent global description of cosmological observations, yet several persistent discrepancies have motivated renewed interest in minimal extensions of the standard framework. The most prominent is the Hubble-constant tension, namely the mismatch between early-time inferences obtained from cosmic microwave background data interpreted within Λ CDM and a variety of late-time determinations based on distance-ladder, tip-of-the-red-giant-branch, and strong-lensing methods. In parallel, recent baryon-acoustic-oscillation analyses, especially when combined with cosmic microwave background information, have revived interest in dynamical dark energy by indicating a preference for time evolution in the dark-energy sector within standard phenomenological parameterizations. A further and partially independent issue is the long-discussed tendency of several late-time weak-lensing and large-scale-structure measurements to favor a lower amplitude of matter clustering than that inferred from early-universe data, although the exact statistical status remains probe-dependent [1–7, 10–14]. The spatially flat Λ CDM model continues to provide an excellent global description of cosmological observations, yet several persistent discrepancies have motivated renewed interest in minimal extensions of the standard framework. The most prominent is the Hubble-constant tension, namely the mismatch between early-time inferences obtained from cosmic microwave background data interpreted within Λ CDM and a variety of late-time determinations based on distance-ladder, tip-of-the-red-giant-branch, and strong-lensing methods. In parallel, recent baryon-acoustic-oscillation analyses, especially when combined with cosmic microwave back-

ground information, have revived interest in dynamical dark energy by indicating a preference for time evolution in the dark-energy sector within standard phenomenological parameterizations. A further and partially independent issue is the long-discussed tendency of several late-time weak-lensing and large-scale-structure measurements to favor a lower amplitude of matter clustering than that inferred from early-universe data, although the exact statistical status remains probe-dependent [1–7, 10–14].

These anomalies are often studied separately, and many proposed resolutions are correspondingly specialized [15, 19–30]. Early-dark-energy constructions are designed primarily to reduce the sound horizon before recombination and thus increase the Hubble constant inferred from the acoustic scale, but they do not automatically generate the preferred low-redshift dark-energy evolution or alleviate the mild clustering tension [15, 19]. Conversely, late-time quintessence models can modify the recent expansion history and suppress the growth of structure, but they do not by themselves produce the pre-recombination sound-horizon shift needed to address the Hubble discrepancy [18, 31–35]. This suggests a sharper question: can one build a single, explicit, and minimal dynamical system that links the early- and late-time phenomena rather than treating them as unrelated ingredients?

The purpose of this paper is to present such a candidate mechanism in the most economical setting possible. We remain entirely within ordinary general relativity, keep the visible and dark matter sectors standard, and introduce only one new degree of freedom: a canonical scalar field with a smooth potential. The potential is constructed so that it contains a localized feature superimposed on a runaway tail. The localized feature is responsible for a transient episode of early dark energy before recombination, while the tail acts as a late-time quintessence sector. In this way, the same scalar field is used to perform three jobs in sequence: first, to in-

*Electronic address: gkouniatis@noa.gr

crease the pre-recombination expansion rate and reduce the sound horizon; second, to redshift away quickly after the early event so as not to disrupt the standard thermal history at later times; and third, to re-emerge at low redshift as a dynamical dark-energy component that weakens linear growth and shifts the phenomenology toward that preferred by recent low-redshift data.

The novelty of the construction is therefore not the use of scalar fields per se, but the specific claim that a single smooth potential can connect the three targets through one continuous dynamical history. At early times, the field is trapped near a localized maximum, furnishing a transient vacuum-like contribution to the energy density. Once the Hubble friction becomes sufficiently weak, the field is released, its excess energy is converted into kinetic motion, and the corresponding energy density rapidly dilutes. At late times, the same field evolves along the tail of the potential and behaves as a thawing quintessence component. This late evolution naturally modifies the recent expansion history and suppresses the growth of matter perturbations relative to Λ CDM, thereby pushing the clustering amplitude downward. The framework is deliberately minimal: there is no modified gravity, no non-minimal coupling, and no interaction introduced in the dark sector.

We derive the background dynamics of the model, identify the local structure of the early feature, obtain a compact relation between the size of the transient early component and the width of the localized bump, show how the sound horizon is reduced at first order, establish the rapid post-release dilution of the field energy density, and demonstrate that the late-time tail produces the sign pattern associated with recent dynamical-dark-energy fits while suppressing linear growth.

II. REVIEW OF THE TENSIONS

Before introducing the model, it is useful to separate clearly the three observational targets that motivate it [12–14, 28]. One concerns the calibration of the cosmic expansion rate through the sound horizon, one concerns the time dependence of the late-time acceleration sector, and one concerns the amplitude of structure growth. A successful unified mechanism must therefore do more than shift one parameter: it must modify the cosmic history in the correct epochs and in the correct directions.

A. The Hubble tension as a sound-horizon problem

The most mature and statistically sharp anomaly is the discrepancy in the Hubble constant. Within flat Λ CDM, early-universe data calibrated by the cosmic microwave background (CMB), especially when combined with external information such as lensing and baryon-acoustic-oscillation measurements, favor a lower value of H_0 than direct late-time determinations based on the lo-

cal distance ladder [1, 2, 4]. Alternative late-time methods, such as tip-of-the-red-giant-branch measurements and strong-lensing time delays, typically lie between the CMB-preferred and SH0ES values, but still tend to remain above the standard early-time anchor [5, 6, 12, 13].

The CMB does not measure H_0 directly. What it measures extremely well is the angular acoustic scale,

$$\theta_* = \frac{r_s(z_*)}{D_A(z_*)}, \quad (2.1)$$

where $r_s(z_*)$ is the comoving sound horizon at last scattering and $D_A(z_*)$ is the angular-diameter distance to the last-scattering surface. The sound horizon is [36, 37]

$$r_s(z_*) = \int_{z_*}^{\infty} \frac{c_s(z)}{H(z)} dz, \quad c_s(z) = \frac{1}{\sqrt{3[1+R(z)]}}. \quad (2.2)$$

Thus the early-time inference of H_0 is tied to the pre-recombination expansion history through r_s . If one increases $H(z)$ before recombination while leaving the rest of the fit under control, then r_s decreases. Since θ_* is tightly measured, a smaller r_s must be compensated mainly by a smaller distance to last scattering, which generally pushes the inferred H_0 upward.

This is why the Hubble tension is, in practice, largely a sound-horizon tension [12–15, 19]. The question is not merely whether one can add energy density to the early universe, but whether one can do so in a localized and sufficiently controlled way: large enough to reduce r_s , early enough to affect the acoustic scale, and transient enough not to spoil the rest of the thermal history. In that sense the tension is highly constraining. It demands a modification near the pre-recombination era, but it also demands that this modification disappear quickly afterward.

B. The dark-energy tension as a history-of-acceleration problem

A second, qualitatively different issue has emerged from recent analyses that combine baryon-acoustic-oscillation information with CMB data and, in some combinations, supernova distances [3, 7, 16, 17]. In the common Chevallier–Polarski–Linder (CPL) description [8, 9],

$$w(a) = w_0 + w_a(1 - a), \quad (2.3)$$

the preferred region is often displaced from the cosmological-constant point $(w_0, w_a) = (-1, 0)$ toward the quadrant

$$w_0 > -1, \quad w_a < 0. \quad (2.4)$$

This is the sign pattern associated with a dark-energy component that is close to a cosmological constant today but was more important in the past than a pure Λ would be [18].

Here the issue is not primarily the sound horizon, but the late-time expansion history. A component with $w > -1$ redshifts more slowly than matter but faster than a true cosmological constant, so for fixed present-day dark-energy density it contributes a larger fraction of the energy budget at intermediate redshift. In other words, it modifies *when* acceleration becomes important and how rapidly the universe interpolates between matter domination and dark-energy domination.

It is important to state the status of this anomaly carefully. The evidence for evolving dark energy is not as settled as the existence of the H_0 discrepancy, and its significance depends on the exact dataset combination and modeling assumptions [3, 7, 16, 17]. Nevertheless, the repeated appearance of the same preferred quadrant is striking enough to motivate model building. For the purposes of the present work, the relevant lesson is operational: if one wants a single mechanism to address current hints in the data, then its late-time behavior should naturally favor $w_0 > -1$ and $w_a < 0$, rather than requiring a finely tuned trajectory that crosses the phantom divide or oscillates artificially.

C. The S_8 tension as a growth-of-structure problem

The third target concerns the amplitude of late-time matter clustering. It is commonly summarized by the parameter

$$S_8 \equiv \sigma_8 \left(\frac{\Omega_{m0}}{0.3} \right)^{1/2}, \quad (2.5)$$

which captures the degeneracy direction to which weak-lensing and low-redshift large-scale-structure surveys are especially sensitive. The broad empirical pattern is that several late-time probes have tended to prefer somewhat smaller clustering amplitudes than the values inferred from CMB-calibrated Λ CDM fits, although the size of the discrepancy is modest and clearly probe-dependent [1, 2, 10, 11].

This tension is physically different from both the H_0 and w_0 - w_a issues. It is not mainly about distances, but about the efficiency with which matter perturbations grow once the primordial fluctuations have been laid down. In general relativity with smooth dark energy, the linear growth factor $D(a)$ obeys [38, 39]

$$D'' + \left(2 + \frac{H'}{H} \right) D' - \frac{3}{2} \Omega_m(a) D = 0, \quad (2.6)$$

where primes denote derivatives with respect to $\ln a$. This equation shows transparently that growth is controlled by two competing effects: the matter fraction drives clustering, while cosmic expansion produces friction. Any mechanism that makes $H(a)$ larger than in Λ CDM during the era of structure formation, or that lowers $\Omega_m(a)$, suppresses the accumulated growth.

That is why late-time quintessence-like behavior tends to lower S_8 [18, 39]. If dark energy is already slightly more important at intermediate redshift than in a pure cosmological-constant model, then the universe expands faster during the growth era and matter has less time to cluster efficiently. The resulting suppression is usually modest, which is appropriate here: the S_8 anomaly is not a dramatic failure of the standard model, but rather a persistent low-level preference in some datasets. A viable mechanism should therefore reduce growth without overcorrecting it.

D. Why these are three separate targets

The three tensions are linked observationally only in the weak sense that they all involve comparisons between early- and late-time inferences. Dynamically, however, they point to different cosmic epochs and different observables:

$$H_0 \text{ tension} \implies \text{pre-recombination } H(z) \text{ and } r_s, \quad (2.7)$$

$$(w_0, w_a) \text{ trend} \implies \text{late-time expansion history}, \quad (2.8)$$

$$S_8 \text{ tension} \implies \text{late-time linear growth}. \quad (2.9)$$

This distinction matters for model building. An early-time modification can reduce the sound horizon and help with H_0 , but by itself it does not guarantee the preferred late-time dark-energy behavior. Conversely, a late-time scalar field can generate $w_0 > -1$, $w_a < 0$, and weaker growth, but it cannot on its own change the pre-recombination sound horizon enough to move the CMB-inferred Hubble constant. The challenge is therefore not to solve one of these problems in isolation, but to construct a single framework that acts in the right way at both early and late times.

This is the perspective adopted in the present paper. We seek one dynamical degree of freedom whose evolution naturally breaks into three stages: a transient pre-recombination energy injection that lowers r_s , a rapid post-event dilution so that standard cosmology is recovered soon afterward, and a late-time quintessence phase that produces $w_0 > -1$, $w_a < 0$, and weaker structure growth. The review above shows why each of these ingredients is required. The next section shows how one smooth scalar potential can realize all of them in a single continuous history.

III. A UNIFIED RESOLUTION

We now show how the model resolves, at the level of explicit background dynamics, the three observational targets reviewed above. The central point is that the mechanism is not a superposition of unrelated fixes. A

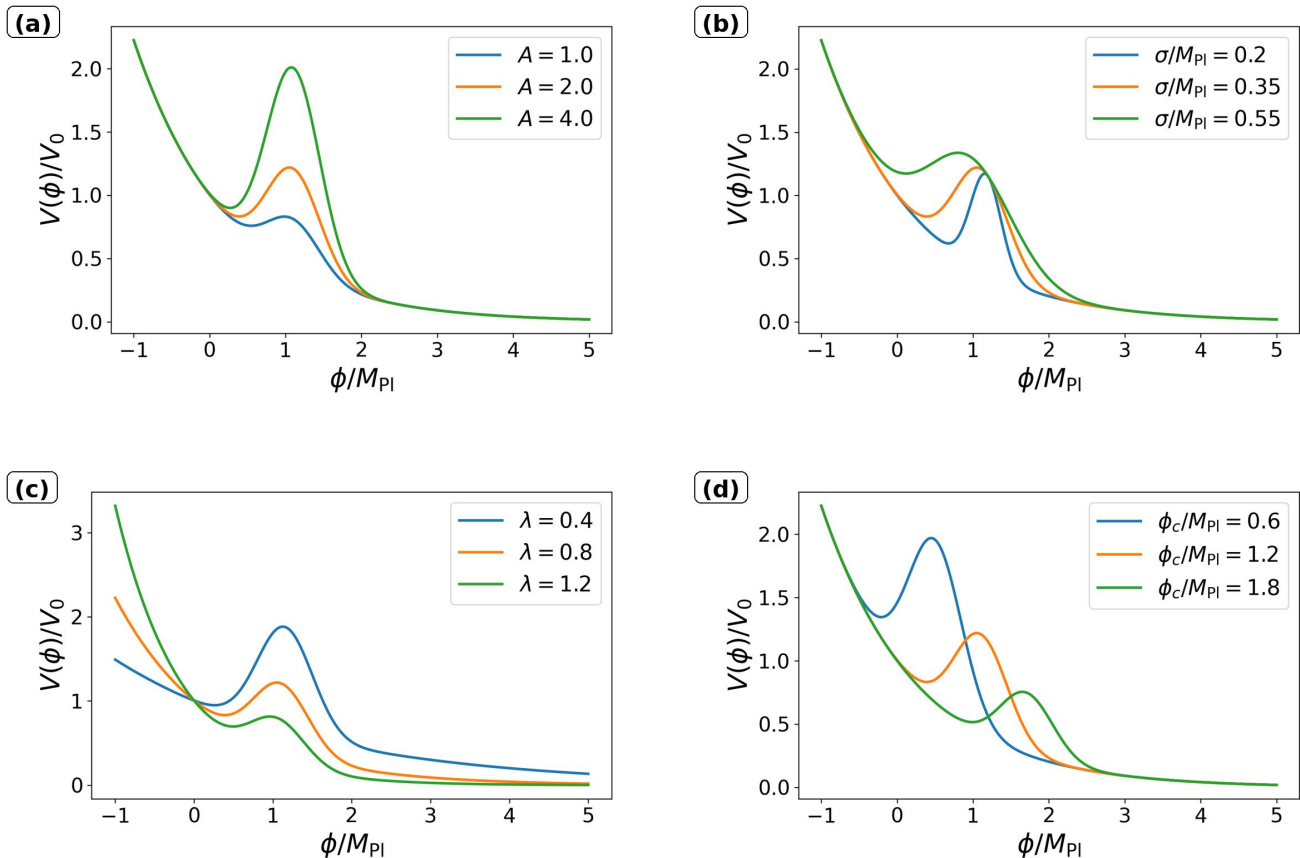


FIG. 1: Square-panel visualization of the bump-tail potential $V(\phi)/V_0$ as a function of ϕ/M_{Pl} , varying one parameter at a time around a common baseline. Panel (a) shows the effect of changing the bump amplitude A , which primarily controls the height of the localized early-time feature and hence the size of the transient early-dark-energy contribution. Panel (b) shows the effect of changing the width σ , which controls how localized or broad the feature is and therefore influences the timing and sharpness of the field release. Panel (c) shows the effect of changing the tail slope λ , which leaves the localized bump intact but changes the steepness of the asymptotic runaway region that governs the late-time quintessence dynamics. Panel (d) shows the effect of changing the bump location ϕ_c , which shifts the feature in field space without altering the basic early/late-time division of roles. Together, the four panels illustrate how one smooth scalar potential can independently control the early-time sound-horizon modification and the late-time dark-energy evolution.

single canonical scalar field evolves through three physically distinct regimes: it first behaves as a transient pre-recombination energy component, then rapidly redshifts away after release from the localized feature, and finally reappears at late times as a quintessence field on the runaway tail. The same degree of freedom therefore acts at exactly the epochs required by the three tensions.

A. One field, one potential, three epochs

The new ingredient is one minimally coupled canonical scalar field ϕ in ordinary general relativity,

$$S = \int d^4x \sqrt{-g} \left[\frac{M_{\text{Pl}}^2}{2} R - \frac{1}{2} g^{\mu\nu} \partial_\mu \phi \partial_\nu \phi - V(\phi) \right] + S_m[g_{\mu\nu}, \psi_i], \quad (3.1)$$

with potential

$$V(\phi) = V_0 e^{-\lambda\phi/M_{\text{Pl}}} \left[1 + A \exp\left(-\frac{(\phi - \phi_c)^2}{2\sigma^2}\right) \right]. \quad (3.2)$$

This form is chosen so that its two factors perform two different physical roles. The Gaussian feature supplies a localized excess in the potential energy and therefore a transient early-dark-energy episode [15, 19]. The exponential tail supplies late-time quintessence [31–35]. The economy of the construction is important. There is no modified gravity, no non-minimal coupling, and no additional dark-sector interaction, in contrast with a number of alternative approaches in the recent literature [20–22, 24–27, 30]. The three tensions are addressed by one continuous scalar trajectory.

To make the content of the model more transparent, it is useful to display the shape of the scalar potential before

discussing the resulting cosmological evolution. Figure 1 shows the bump-tail potential for representative variations of its four defining parameters. The figure makes clear that the model separates naturally into two sectors of physical relevance. The localized Gaussian feature, governed mainly by A , σ , and ϕ_c , controls the transient early-time energy injection, while the exponential factor, governed by λ , controls the steepness of the late-time runaway tail and therefore the quintessence behavior. In this way the same smooth potential is able to encode both the pre-recombination modification relevant for the sound horizon and the late-time evolution relevant for dark energy and structure growth.

At early times the field is held in place by Hubble friction near the crest of the localized bump. In that regime its energy density is potential dominated and nearly vacuum-like, so it temporarily increases the expansion rate. Once the Hubble rate drops enough that the field can respond to the negative curvature of the bump, it rolls off, converts its stored potential energy into kinetic energy, and dilutes extremely rapidly. Much later, when the field has reached the smooth exponential tail, it behaves as an ordinary quintessence component and modifies the recent expansion history and the growth of structure.

B. Early-time resolution of the Hubble tension

The H_0 tension is fundamentally a pre-recombination problem because the CMB does not directly measure H_0 , it measures the acoustic scale [1, 2, 36, 37]

$$\theta_* = \frac{r_s(z_*)}{D_A(z_*)}, \quad (3.3)$$

where $r_s(z_*)$ is the sound horizon at last scattering. To increase the CMB-inferred value of H_0 , one must reduce r_s without spoiling the overall fit to the acoustic structure. This requires a temporary increase in the expansion rate before recombination.

That is precisely what the bump in Eq. (3.2) provides. Near the local maximum $\phi = \phi_*$, the field is approximately frozen and its energy density is dominated by the local potential height,

$$\rho_\phi \simeq V_*, \quad V_* \equiv V(\phi_*). \quad (3.4)$$

The local curvature at the crest is negative and, in the bump-dominated regime, takes the simple form

$$V_{,\phi\phi}(\phi_*) \simeq -\frac{V_*}{\sigma^2}. \quad (3.5)$$

The field remains stuck there as long as Hubble friction dominates over the local instability. Release occurs when these two scales become comparable,

$$3H_c \simeq \sqrt{|V_{,\phi\phi}(\phi_*)|} \quad \implies \quad H_c^2 \simeq \frac{V_*}{9\sigma^2}. \quad (3.6)$$

This relation shows that the width σ of the feature controls the epoch at which the transient is activated.

At the moment of release the scalar fraction is

$$f_{\text{EDE}} \equiv \frac{\rho_\phi}{3M_{\text{Pl}}^2 H^2} \Big|_{\text{peak}} \simeq \frac{V_*}{3M_{\text{Pl}}^2 H_c^2} \simeq 3 \frac{\sigma^2}{M_{\text{Pl}}^2}. \quad (3.7)$$

This is one of the key relations in the model: the peak early-dark-energy fraction is set directly by the field-space width of the bump. In other words, the amount of pre-recombination energy injection is not inserted by hand as an abstract fluid parameter; it is tied directly to the geometry of the scalar potential.

During the transient, the total Hubble rate is larger than in Λ CDM. Writing the early scalar contribution as a fraction $f_{\text{EDE}}(z)$, one has schematically

$$H^2(z) = \frac{H_{\Lambda\text{CDM}}^2(z)}{1 - f_{\text{EDE}}(z)}. \quad (3.8)$$

Since the sound horizon is

$$r_s(z_*) = \int_{z_*}^{\infty} \frac{c_s(z)}{H(z)} dz, \quad (3.9)$$

a positive localized f_{EDE} necessarily decreases r_s . To first order,

$$\frac{\Delta r_s}{r_s} \simeq -\frac{1}{2} \langle f_{\text{EDE}} \rangle_{r_s} < 0. \quad (3.10)$$

This sign is the essential result. A transient pre-recombination energy excess makes the sound horizon smaller. Because the acoustic angle θ_* is measured so precisely, a smaller sound horizon pushes the CMB-inferred value of H_0 upward [15, 19]. The model therefore addresses the Hubble tension in the physically correct way: not by modifying late-time distances alone, but by changing the pre-recombination standard ruler itself.

Figure 2 provides a compact visual summary of how the scalar sector modifies the position of the cosmological model in the H_0 - r_d plane relative to the standard Λ CDM case. In the scalar-absent limit, the model remains close to the conventional low- H_0 , high- r_d region, represented by the Λ CDM point. Once the scalar field becomes effective, however, the model follows a well-defined trajectory toward higher values of H_0 and lower values of r_d . This is precisely the direction that is phenomenologically relevant for alleviating the Hubble tension, since late-time measurements tend to prefer a larger Hubble constant, whereas BAO measurements can remain compatible provided the sound horizon is correspondingly reduced. The four panels show that several representative scalar-field parameter choices lie substantially closer than Λ CDM to the observationally preferred regions, especially for Pantheon+ and TDCOSMO 2025, while also moving in the correct direction relative to the DESI DR2 BAO band. The DES-SN5YR panel should be interpreted more qualitatively, as supernova data primarily constrain the late-time expansion history rather than directly determining

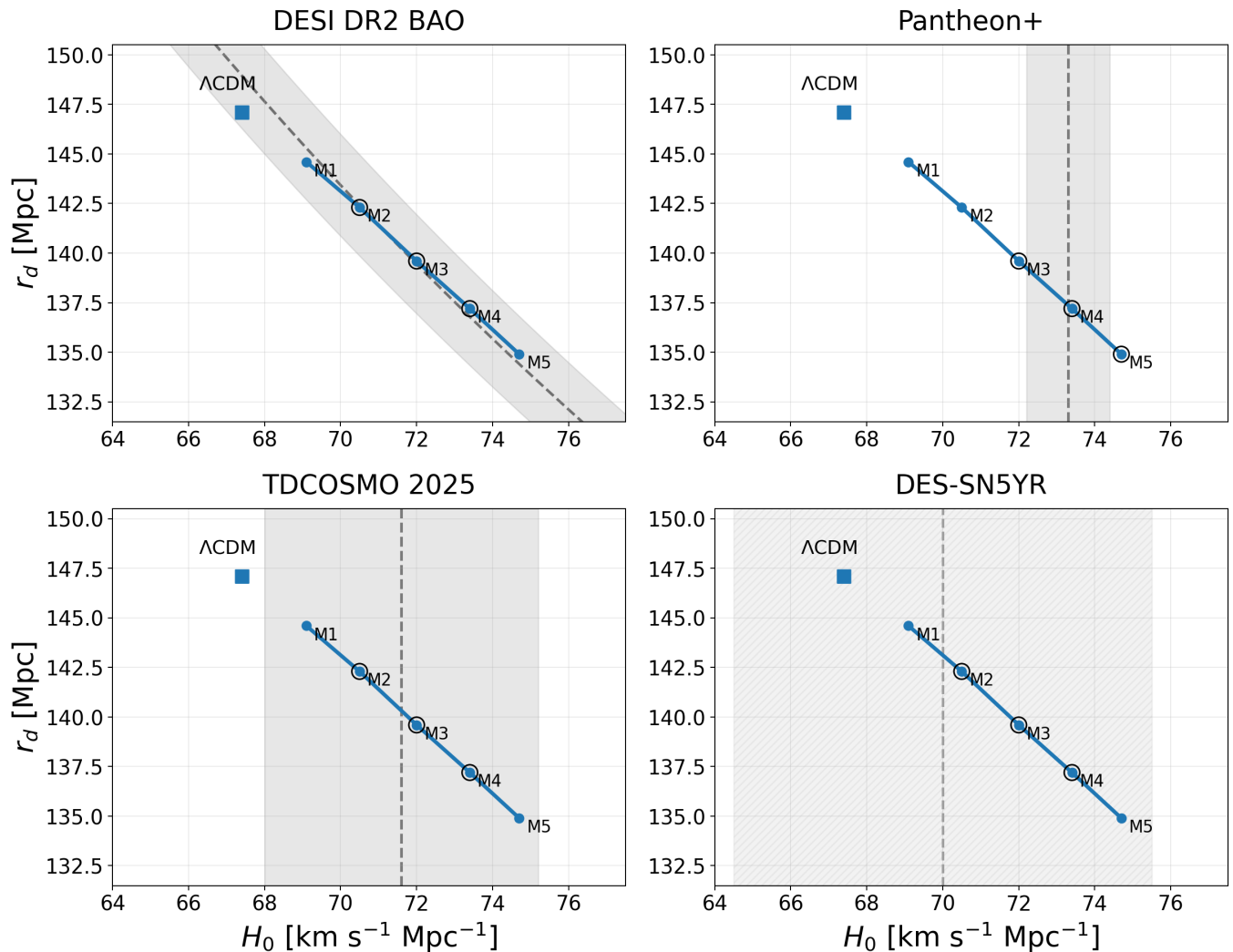


FIG. 2: Comparison in the H_0 - r_d plane between the standard Λ CDM scenario and the scalar-effective cosmology considered in this work, shown against four observational directions: DESI DR2 BAO [7], Pantheon+ [16], TDCOSMO 2025 [6], and DES-SN5YR [17]. The square denotes the scalar-absent case, namely the usual Λ CDM reference point, while the connected circular markers $M1$ - $M5$ represent a sequence of representative scalar-present parameter choices of the bump-tail potential. For the plotted scalar-present points we used $M1$: $(A, \sigma, \lambda, \phi_c) = (1.4, 0.22, 0.45, 0.90)$, $M2$: $(1.9, 0.28, 0.60, 1.10)$, $M3$: $(2.5, 0.34, 0.75, 1.25)$, $M4$: $(3.2, 0.41, 0.90, 1.40)$, and $M5$: $(4.0, 0.50, 1.05, 1.60)$. Moving along this sequence shifts the cosmological prediction toward larger H_0 and smaller r_d , which is the characteristic direction required to ease the Hubble tension. The shaded regions indicate the observational preference directions in each panel: a diagonal band for BAO, reflecting the approximate $H_0 r_d$ degeneracy, and vertical bands for the late-time probes, which preferentially favor larger values of H_0 . The highlighted scalar-field points indicate the parameter choices that are visually closest to the preferred observational regions in each panel. The figure is intended as an illustrative comparison of the direction of the shift induced by the scalar field, rather than as the result of a full likelihood analysis.

r_d , but it still shows that the scalar-effective solutions are more naturally aligned with the late-time high- H_0 trend than the standard scalar-absent case. In this sense, the figure illustrates the main point of the model: the scalar field introduces a correlated shift in (H_0, r_d) that is much better suited to the current observational landscape than ordinary Λ CDM.

C. Why the early excess does not overclose the universe

Any early-dark-energy mechanism must answer a second question just as clearly: why does the extra component not remain important after it has done its job? In the present model the answer is dynamical and automatic [15, 19].

Once the field rolls off the bump, its excess potential energy is converted into motion along the tail. Immedi-

ately after release there is generically a period in which the kinetic energy dominates,

$$\dot{\phi}^2 \gg V(\phi). \quad (3.11)$$

The Klein–Gordon equation then reduces to

$$\ddot{\phi} + 3H\dot{\phi} \simeq 0, \quad (3.12)$$

whose solution is

$$\dot{\phi} \propto a^{-3}. \quad (3.13)$$

Therefore the scalar energy density redshifts as

$$\rho_\phi \simeq \frac{1}{2}\dot{\phi}^2 \propto a^{-6}. \quad (3.14)$$

This is much faster than radiation and vastly faster than matter. The field undergoes a brief kination phase and gets out of the way almost immediately. This is crucial for viability: the same mechanism that temporarily raises $H(z)$ before recombination also guarantees that the early excess is not a persistent contaminant of the later thermal history.

D. Late-time resolution of the dark-energy tension

Far from the localized bump, the potential reduces to the exponential tail [31–35],

$$V(\phi) \rightarrow V_{\text{tail}}(\phi) = V_0 e^{-\lambda\phi/M_{\text{Pl}}}. \quad (3.15)$$

At late times this is a standard quintessence regime. The field rolls slowly enough that

$$3H\dot{\phi} + V_{,\phi} \simeq 0, \quad V_{,\phi} = -\frac{\lambda}{M_{\text{Pl}}}V. \quad (3.16)$$

In the dark-energy-dominated regime this implies

$$1 + w_\phi \simeq \frac{\lambda^2}{3} \Omega_{\text{DE}}. \quad (3.17)$$

The immediate physical consequence is that

$$w_\phi > -1 \quad (\lambda \neq 0). \quad (3.18)$$

Thus the model naturally produces a non-phantom dark-energy sector. This is exactly the direction favored by the recent w_0 – w_a fits: the late-time acceleration is not a strict cosmological constant, but a slowly evolving quintessence-like component [3, 7, 16–18].

The sign of w_a is equally transparent. In the CPL parametrization,

$$w(a) = w_0 + w_a(1 - a), \quad w_a = -\left. \frac{dw}{d \ln a} \right|_{a=1}. \quad (3.19)$$

For quintessence on the tail, the dark-energy fraction increases toward the present, and one finds

$$\frac{d\Omega_{\text{DE}}}{d \ln a} = -3w_\phi \Omega_{\text{DE}}(1 - \Omega_{\text{DE}}) > 0, \quad (3.20)$$

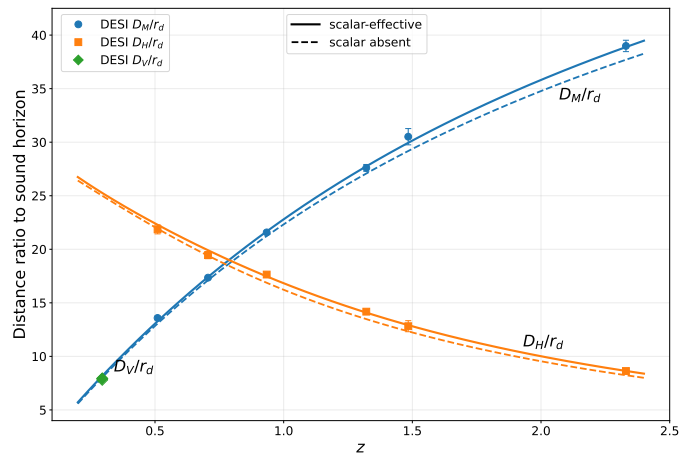


FIG. 3: DESI BAO distance measurements compared with a scalar-effective cosmology and with a counterfactual model in which the scalar contribution is removed. Filled markers denote the DESI measurements of D_M/r_d , D_H/r_d , and D_V/r_d , while the solid curves show the scalar-effective prediction. The dashed curves show the corresponding background evolution when the scalar is absent, keeping the same matter density and Hubble scale but restoring a standard late-time Λ CDM expansion and sound horizon. The separation between the solid and dashed curves makes explicit the deviation induced by the scalar sector across the DESI redshift range.

because $-1 < w_\phi < 0$. Using Eq. (3.17), it follows that

$$\frac{dw_\phi}{d \ln a} > 0 \quad \implies \quad w_a < 0. \quad (3.21)$$

So the characteristic sign pattern

$$w_0 > -1, \quad w_a < 0 \quad (3.22)$$

is not imposed by hand; it is the natural late-time behavior of the same scalar field after the early transient has passed.

At the present epoch, the slow-roll estimate becomes

$$1 + w_0 \simeq \frac{\lambda^2}{3} \Omega_{\text{DE},0}, \quad w_a \simeq -\lambda^2 \Omega_{\text{DE},0}(1 - \Omega_{\text{DE},0}). \quad (3.23)$$

These expressions show the role of the tail slope λ : it controls how strongly the model departs from Λ CDM at late times, and therefore how far one moves into the empirically preferred w_0 – w_a quadrant.

Figure 3 presents a direct comparison between the DESI BAO distance ratios and the background expansion predicted by the scalar scenario considered in this work [7]. The solid curves represent the scalar-effective model, whereas the dashed curves show the corresponding evolution obtained after removing the scalar contribution. In this way, the figure isolates the role of the scalar field in shifting the comoving angular-diameter distance, the Hubble distance, and the isotropic BAO distance scale. The close tracking of the DESI points by the

scalar-effective curves, together with the visible displacement of the scalar-absent case, highlights that the scalar sector is responsible for the improved agreement with the observed BAO expansion history.

E. Late-time suppression of growth and the shift in S_8

The same tail that modifies the background expansion also reduces the growth of matter perturbations. This is the third and final job required of the model [39].

In general relativity with smooth dark energy, the linear growth factor $D(a)$ obeys [38, 39]

$$D'' + \left(2 + \frac{H'}{H}\right) D' - \frac{3}{2} \Omega_m(a) D = 0, \quad (3.24)$$

where primes denote derivatives with respect to $\ln a$. This equation makes the physics transparent. Growth is stronger when the matter fraction is larger and weaker when the expansion rate is larger.

For the present model, the tail satisfies $w_\phi > -1$. Therefore, for fixed present-day dark-energy density, the scalar contributed more energy in the past than a true cosmological constant would have:

$$\rho_\phi(a) = \rho_{\phi 0} \exp\left[3 \int_a^1 \frac{1 + w_\phi(\tilde{a})}{\tilde{a}} d\tilde{a}\right] > \rho_{\Lambda 0} \quad (a < 1). \quad (3.25)$$

It follows that

$$H(a) > H_{\Lambda\text{CDM}}(a), \quad \Omega_m(a) < \Omega_m^{\Lambda\text{CDM}}(a), \quad (a < 1). \quad (3.26)$$

Both effects in Eq. (3.24) act in the same direction: they suppress growth relative to ΛCDM . Matter has less time to cluster, and the effective gravitational source term is reduced because the matter fraction is smaller during the era when structures are forming.

Since

$$S_8 \equiv \sigma_8 \left(\frac{\Omega_{m0}}{0.3}\right)^{1/2}, \quad (3.27)$$

one may write schematically

$$\frac{\Delta S_8}{S_8} = \frac{\Delta D(1)}{D(1)} + \frac{1}{2} \frac{\Delta \Omega_{m0}}{\Omega_{m0}}. \quad (3.28)$$

In the present model the late tail gives $\Delta D(1) < 0$, and the preferred late-time fit typically also moves toward smaller Ω_{m0} [10, 11]. Both effects lower S_8 . There is also a secondary suppression channel from the brief post-bump kination era of Eq. (3.14): during that stage the expansion rate is temporarily enhanced while the scalar does not cluster like matter, which slightly reduces the accumulated growth even further. The main effect, however, is the late-time quintessence tail.

To make the growth-sector effect more explicit, Fig. 4 shows the redshift evolution of $f\sigma_8(z)$ for the scalar-effective cosmology and for a corresponding scalar-absent

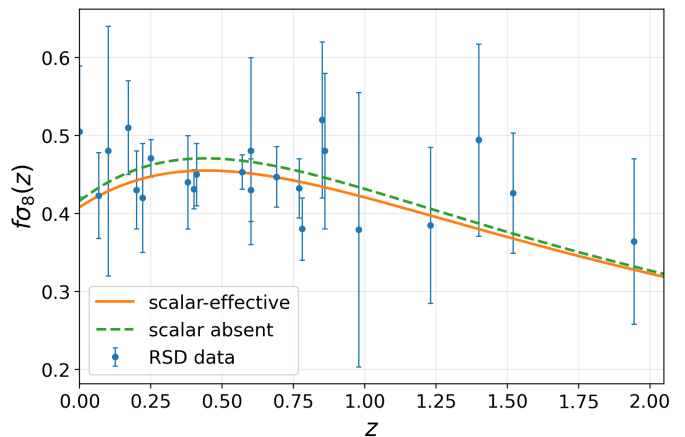


FIG. 4: Late-time growth history in the bump-tail scalar scenario, shown through the observable $f\sigma_8(z)$. The solid curve denotes a scalar-effective late-time proxy constructed with $\Omega_{m0} = 0.30$, $\sigma_8^{\Lambda\text{CDM}}(0) = 0.811$, and tail slope $\lambda = 0.60$, which yields the effective CPL parameters $w_0 = -0.916$ and $w_a = -0.0756$. The dashed curve shows the corresponding scalar-absent reference evolution, while the points are representative redshift-space-distortion (RSD) measurements of $f\sigma_8$. The downward displacement of the scalar-effective curve relative to the scalar-absent case illustrates the suppression of linear growth produced by the late-time scalar tail.

reference case. This plot provides the visual counterpart of the analytic argument developed above. In the present model, the late-time tail behaves as a quintessence component with $w_\phi > -1$, so for fixed present-day dark-energy density the scalar contributes more energy at intermediate redshift than a true cosmological constant. As a result, the expansion history is enhanced and the matter fraction is reduced during the era of structure formation. Both effects act in the same direction in the linear growth equation, suppressing the growth factor relative to the scalar-absent case. The figure therefore illustrates directly why the model moves the predicted clustering amplitude downward, in the direction preferred by low-redshift constraints on S_8 [10, 11].

IV. CONCLUSIONS

In this work we have presented a concrete single-field framework that addresses, within ordinary general relativity, three of the most widely discussed tensions in cosmology. The central idea is simple but nontrivial in its implementation: one canonical scalar field, evolving in a smooth bump-tail potential, can modify the cosmic history in the two epochs where the standard ΛCDM description is currently under the greatest phenomenological pressure. A localized feature in the potential generates a transient pre-recombination energy injection, while the asymptotic tail drives late-time quintessence. The same field therefore acts first as an early dark energy

component and later as a dynamical dark energy component.

The physical logic of the construction is transparent. During the early phase, the field is temporarily held near the localized feature, increasing the expansion rate before recombination and thereby reducing the sound horizon. This moves the CMB-inferred value of the Hubble constant upward, in the direction required to ease the H_0 tension. After the release from the feature, the field rapidly enters a regime of fast dilution, so the early energy excess does not remain as an unwanted contribution at later times. Finally, on the tail of the potential, the field behaves as a quintessence sector with a mildly evolving equation of state. This naturally produces the sign pattern favored by recent late-time analyses, namely $w_0 > -1$ and $w_a < 0$, while also suppressing the growth of matter perturbations and lowering the predicted clustering amplitude in the direction preferred by low-redshift weak-lensing and large-scale-structure data.

The main result of the paper is therefore not merely that each of the three tensions can be influenced by scalar dynamics, which is already well known in more specialized contexts, but that a single smooth potential can produce all three effects in one continuous cosmological history. The early bump controls the transient pre-recombination modification relevant for the sound horizon, and the late tail controls the subsequent dark-energy evolution and the suppression of structure growth. In this sense, the model provides a unified and analytically

tractable candidate resolution of the H_0 , w_0 - w_a , and S_8 anomalies.

There are several natural directions for future work. The first is the perturbative and numerical program, which is necessary to determine the quantitatively allowed region of parameter space. A second is to study in greater detail the microphysical origin of the bump-tail potential and the degree of tuning, if any, required to realize the desired cosmic history. A third and especially interesting possibility is to investigate whether the same scalar field considered here could also play the role of the inflaton in the very early universe [40–48]. In other words, it is worth examining whether the present framework can be embedded into a still more unified picture in which inflation, the transient early-dark-energy episode, and late-time quintessence all arise from one and the same dynamical degree of freedom. We leave this question for future work.

The current cosmological tensions may or may not ultimately survive as evidence for new physics, but if they do, the required new physics need not be baroque. It is possible, at least at the level of controlled analytic dynamics, for one minimally coupled scalar field in standard general relativity to leave distinct and potentially observable imprints across widely separated epochs of cosmic history. Whether nature actually makes use of such an economy remains to be determined by forthcoming data and by the more complete phenomenological analysis that this model now motivates.

-
- [1] N. Aghanim *et al.* [Planck Collaboration], *Planck 2018 results. VI. Cosmological parameters*, *Astron. Astrophys.* **641**, A6 (2020), [arXiv:1807.06209 \[astro-ph.CO\]](#).
 - [2] T. Louis *et al.* [ACT Collaboration], *DR6 Power Spectra, Likelihoods and Λ CDM Parameters*, [arXiv:2503.14452 \[astro-ph.CO\]](#).
 - [3] E. Calabrese *et al.* [ACT Collaboration], *DR6 Constraints on Extended Cosmological Models*, [arXiv:2503.14454 \[astro-ph.CO\]](#).
 - [4] A. G. Riess *et al.*, *A Comprehensive Measurement of the Local Value of the Hubble Constant with 1 km s⁻¹ Mpc⁻¹ Uncertainty from the Hubble Space Telescope and the SH0ES Team*, *Astrophys. J. Lett.* **934**, L7 (2022), [arXiv:2112.04510 \[astro-ph.CO\]](#).
 - [5] W. L. Freedman, B. F. Madore, I. S. Jang, T. J. Hoyt, A. J. Lee and K. A. Owens, *Status Report on the Chicago-Carnegie Hubble Program (CCHP): Three Independent Astrophysical Determinations of the Hubble Constant Using the James Webb Space Telescope*, *Astrophys. J.* **985**, 203 (2025), [arXiv:2408.06153 \[astro-ph.CO\]](#).
 - [6] S. Birrer *et al.* [TDCOSMO Collaboration], *TDCOSMO 2025: Cosmological constraints from strong lensing time delays*, *Astron. Astrophys.* **704**, A63 (2025), [arXiv:2506.03023 \[astro-ph.CO\]](#).
 - [7] M. Abdul Karim *et al.* [DESI Collaboration], *DESI DR2 Results II: Measurements of Baryon Acoustic Oscillations and Cosmological Constraints*, *Phys. Rev. D* **112**, 083515 (2025), [arXiv:2503.14738 \[astro-ph.CO\]](#).
 - [8] M. Chevallier and D. Polarski, *Accelerating Universes with Scaling Dark Matter*, *Int. J. Mod. Phys. D* **10**, 213 (2001), [arXiv:gr-qc/0009008](#).
 - [9] E. V. Linder, *Exploring the Expansion History of the Universe*, *Phys. Rev. Lett.* **90**, 091301 (2003), [arXiv:astro-ph/0208512](#).
 - [10] T. M. C. Abbott *et al.* [DES Collaboration], *Dark Energy Survey Year 6 Results: Cosmological Constraints from Cosmic Shear*, [arXiv:2602.10065 \[astro-ph.CO\]](#).
 - [11] A. H. Wright *et al.*, *KiDS-Legacy: Cosmological constraints from cosmic shear with the complete Kilo-Degree Survey*, *Astron. Astrophys.* **703**, A158 (2025), [arXiv:2503.19441 \[astro-ph.CO\]](#).
 - [12] L. Verde, T. Treu and A. G. Riess, *Tensions between the Early and the Late Universe*, *Nature Astron.* **3**, 891 (2019), [arXiv:1907.10625 \[astro-ph.CO\]](#).
 - [13] L. Knox and M. Millea, *Hubble constant hunter's guide*, *Phys. Rev. D* **101**, 043533 (2020), [arXiv:1908.03663 \[astro-ph.CO\]](#).
 - [14] E. Di Valentino, O. Mena, S. Pan, L. Visinelli, W. Yang, A. Melchiorri, D. F. Mota, A. G. Riess and J. Silk, *In the Realm of the Hubble tension – a Review of Solutions*, *Class. Quant. Grav.* **38**, 153001 (2021), [arXiv:2103.01183 \[astro-ph.CO\]](#).
 - [15] V. Poulin, T. L. Smith, T. Karwal and M. Kamionkowski, *Early Dark Energy Can Resolve the Hubble Tension*, *Phys. Rev. Lett.* **122**, 221301 (2019), [arXiv:1811.04083 \[astro-ph.CO\]](#).

- [16] D. Brout *et al.*, *The Pantheon+ Analysis: Cosmological Constraints*, *Astrophys. J.* **938**, 110 (2022), [arXiv:2202.04077 \[astro-ph.CO\]](#).
- [17] T. M. C. Abbott *et al.* [DES Collaboration], *The Dark Energy Survey: Cosmology Results With ~ 1500 New High-redshift Type Ia Supernovae Using The Full 5-year Dataset*, *Astrophys. J. Lett.* **973**, L14 (2024), [arXiv:2401.02929 \[astro-ph.CO\]](#).
- [18] R. R. Caldwell and E. V. Linder, *The Limits of Quintessence*, *Phys. Rev. Lett.* **95**, 141301 (2005), [arXiv:astro-ph/0505494 \[astro-ph\]](#).
- [19] V. Poulin, T. L. Smith and T. Karwal, *The Ups and Downs of Early Dark Energy solutions to the Hubble tension: a review of models, hints and constraints circa 2023*, *Phys. Dark Univ.* **42**, 101348 (2023), [arXiv:2302.09032 \[astro-ph.CO\]](#).
- [20] M. Petronikolou, S. Basilakos and E. N. Saridakis, *Alleviating H_0 tension in Horndeski gravity*, *Phys. Rev. D* **106**, 124051 (2022), [arXiv:2110.01338 \[gr-qc\]](#).
- [21] S. Banerjee, M. Petronikolou and E. N. Saridakis, *Alleviating H_0 Tension with New Gravitational Scalar Tensor Theories*, *Phys. Rev. D* **108**, 024012 (2023), [arXiv:2209.02426 \[gr-qc\]](#).
- [22] M. Petronikolou and E. N. Saridakis, *Alleviating the H_0 Tension in Scalar-Tensor and Bi-Scalar-Tensor Theories*, *Universe* **9**, 397 (2023), [arXiv:2308.16044 \[gr-qc\]](#).
- [23] G. Kouniatalis and E. N. Saridakis, *A null test of the Hubble tension*, (2026), [arXiv:2601.22043 \[astro-ph.CO\]](#).
- [24] S. Nojiri, S. D. Odintsov and V. K. Oikonomou, *Integral $F(R)$ Gravity and Saddle Point Condition as a Remedy for the H_0 -tension*, *Nucl. Phys. B* **980**, 115850 (2022), [arXiv:2205.11681 \[gr-qc\]](#).
- [25] S. D. Odintsov, V. K. Oikonomou and G. S. Sharov, *Early dark energy with power-law $F(R)$ gravity*, *Phys. Lett. B* **843**, 137988 (2023), [arXiv:2305.17513 \[gr-qc\]](#).
- [26] X. Ren, S.-F. Yan, Y. Zhao, Y.-F. Cai and E. N. Saridakis, *Gaussian processes and effective field theory of $f(T)$ gravity under the H_0 tension*, *Astrophys. J.* **932**, 131 (2022), [arXiv:2203.01926 \[astro-ph.CO\]](#).
- [27] S. Basilakos, A. Lymperis, M. Petronikolou and E. N. Saridakis, *Alleviating both H_0 and σ_8 tensions in Tsallis cosmology*, *Eur. Phys. J. C* **84**, 297 (2024), [arXiv:2308.01200 \[gr-qc\]](#).
- [28] E. Di Valentino, J. L. Said and E. N. Saridakis, *Cosmological tensions in the era of precision cosmology: Insights from Tensions in Cosmology 2025*, [arXiv:2509.25288 \[astro-ph.CO\]](#).
- [29] T. Papanikolaou, *The H_0 tension alleviated through ultra-light primordial black holes: an information insight through gravitational waves*, *PoS CORFU2022*, 265 (2023), [arXiv:2303.00600 \[astro-ph.CO\]](#).
- [30] C. G. Boiza, M. Petronikolou, M. Bouhmadi-López and E. N. Saridakis, *Addressing H_0 and S_8 tensions within $f(Q)$ cosmology*, *JCAP* **12**, 011 (2025), [arXiv:2505.18264 \[astro-ph.CO\]](#).
- [31] C. Wetterich, *Cosmology and the Fate of Dilatation Symmetry*, *Nucl. Phys. B* **302**, 668 (1988).
- [32] B. Ratra and P. J. E. Peebles, *Cosmological Consequences of a Rolling Homogeneous Scalar Field*, *Phys. Rev. D* **37**, 3406 (1988).
- [33] P. G. Ferreira and M. Joyce, *Cosmology with a Primordial Scaling Field*, *Phys. Rev. D* **58**, 023503 (1998), [arXiv:astro-ph/9711102](#).
- [34] E. J. Copeland, A. R. Liddle and D. Wands, *Exponential Potentials and Cosmological Scaling Solutions*, *Phys. Rev. D* **57**, 4686 (1998), [arXiv:gr-qc/9711068](#).
- [35] E. J. Copeland, M. Sami and S. Tsujikawa, *Dynamics of dark energy*, *Int. J. Mod. Phys. D* **15**, 1753 (2006), [arXiv:hep-th/0603057](#).
- [36] W. Hu and N. Sugiyama, *Small scale cosmological perturbations: An analytic approach*, *Astrophys. J.* **444**, 489 (1995), [arXiv:astro-ph/9407093](#).
- [37] D. J. Eisenstein and W. Hu, *Baryonic Features in the Matter Transfer Function*, *Astrophys. J.* **496**, 605 (1998), [arXiv:astro-ph/9709112](#).
- [38] P. J. E. Peebles, *The Large-Scale Structure of the Universe*, Princeton University Press, Princeton (1980).
- [39] E. V. Linder, *Cosmic growth history and expansion history*, *Phys. Rev. D* **72**, 043529 (2005), [arXiv:astro-ph/0507263](#).
- [40] A. A. Starobinsky, *A new type of isotropic cosmological models without singularity*, *Phys. Lett. B* **91**, 99 (1980), [doi:10.1016/0370-2693\(80\)90670-X](#).
- [41] A. H. Guth, *Inflationary universe: A possible solution to the horizon and flatness problems*, *Phys. Rev. D* **23**, 347 (1981), [doi:10.1103/PhysRevD.23.347](#).
- [42] A. D. Linde, *A new inflationary universe scenario: A possible solution of the horizon, flatness, homogeneity, isotropy and primordial monopole problems*, *Phys. Lett. B* **108**, 389 (1982), [doi:10.1016/0370-2693\(82\)91219-9](#).
- [43] A. Albrecht and P. J. Steinhardt, *Cosmology for Grand Unified Theories with Radiatively Induced Symmetry Breaking*, *Phys. Rev. Lett.* **48**, 1220 (1982), [doi:10.1103/PhysRevLett.48.1220](#).
- [44] A. D. Linde, *Chaotic inflation*, *Phys. Lett. B* **129**, 177 (1983), [doi:10.1016/0370-2693\(83\)90837-7](#).
- [45] G. Kouniatalis and E. N. Saridakis, *Inflation from a generalized exponential plateau: towards extra suppressed tensor-to-scalar ratios*, *JCAP* **11**, 038 (2025), [arXiv:2507.17721 \[astro-ph.CO\]](#).
- [46] G. Kouniatalis, *The Wave Function of the Universe and Inflation*, (2025), [arXiv:2510.04775 \[gr-qc\]](#).
- [47] V. Mukhanov, *Physical Foundations of Cosmology*, Cambridge University Press, Cambridge (2005).
- [48] A. R. Liddle and D. H. Lyth, *Cosmological Inflation and Large-Scale Structure*, Cambridge University Press, Cambridge (2000).